

## Taming chaos by impurities in two-dimensional oscillator arrays

M. Weiss, Tsampikos Kottos, and T. Geisel

Max-Planck-Institut für Strömungsforschung, and Institut für Nichtlineare Dynamik der Universität Göttingen, Bunsenstraße 10,  
D-37073 Göttingen, Germany

(Received 10 January 2001; published 19 April 2001)

The effect of impurities in a two-dimensional lattice of coupled nonlinear chaotic oscillators and their ability to control the dynamical behavior of the system are studied. We show that a single impurity can produce synchronized spatiotemporal patterns, even though all oscillators and the impurity are chaotic when uncoupled. When a small number of impurities is arranged in a way, that the lattice is divided into two disjoint parts, synchronization is enforced even for small coupling. The synchronization is not affected as the size of the lattice increases, although the impurity concentration tends to zero.

DOI: 10.1103/PhysRevE.63.056211

PACS number(s): 05.45.-a, 05.30.-d, 05.40.-a, 73.21.-b

### I. INTRODUCTION

Coupled arrays of oscillators are studied extensively in many fields of science because of their prevalence in nature. They are used as models for coupled arrays of neurons [1], chemical reactions [2], coupled lasers [3] or Josephson junctions [4], charge-density-wave conductors [5], crystal dislocations in metals [6], and proton conductivity in hydrogen-bonded chains [7]. Various models and coupling schemes have been proposed and analyzed previously [8]. A particular class are arrays of coupled oscillators, which exhibit chaotic motion when uncoupled. This class includes the forced Frenkel-Kontorova model [9], which finds a straightforward physical realization in an array of diffusively coupled Josephson junctions [10,11], in which the applied current of each junction is modulated by a common frequency. The possibility to obtain synchronized motion in such systems has been investigated recently by Braiman *et al.* for the case of one- (1D) and two-dimensional (2D) chaotic arrays of forced damped nonlinear pendula [12] and coupled Josephson junctions [13]. They observed the emergence of complex but frequency-locked spatiotemporal patterns, in which the chaotic behavior was completely suppressed, when a certain amount of *disorder* had been introduced by randomizing the lengths of the pendula. In Ref. [14], the same phenomenon has been investigated from a completely different point of view: It was shown for 1D arrays of coupled chaotic pendula that introducing a single impurity at a particular site is sufficient to lead to complete synchronization.

In this paper, we study 2D arrays of coupled chaotic pendula. We ask for the minimal coupling as well as the influence of concentration and arrangement of impurities needed to observe spatiotemporal patterns. Although for geometrical reasons one might expect that a single impurity cannot play the role it plays in 1D arrays, we find that it is able to tame the chaotic behavior of an arbitrarily large 2D array, provided that the coupling is strong enough. A single impurity can produce synchronized spatiotemporal patterns, even though all oscillators and the impurity are chaotic when uncoupled. In order to observe spatiotemporal patterns for smaller couplings, the geometrical arrangement of the impurities is shown to play a crucial role. Specifically, we show that an impurity configuration that divides the lattice into at least two disjoint parts is most appropriate for the creation of

synchronized solutions. Such configurations will always produce patterns that locally can be identified as lines, provided the coupling is above a threshold value. The resulting spatiotemporal patterns are stable with respect to an increase of the system size, indicating that an impurity concentration that tends to zero may suffice to lead to synchronization.

### II. MODEL

We will focus our analysis on the model examined in Refs. [12,14]:

$$l_{n,m}^2 \ddot{\theta}_{n,m} + \gamma \dot{\theta}_{n,m} = -g l_{n,m} \sin \theta_{n,m} + \tau' + \tau \sin \omega t + k(\theta_{n+1,m} + \theta_{n-1,m} - 4\theta_{n,m} + \theta_{n,m+1} + \theta_{n,m-1}), \quad (1)$$

where  $n, m = 1, 2, \dots, N$ . Thus, there is a damped, driven pendulum with unity mass and length  $l_{n,m}$  on each site  $(n, m)$  of the lattice, subject to an ac and a dc torque. The parameters used are the gravitational acceleration  $g=1$ , the dc torque  $\tau'=0.7155$ , the ac torque  $\tau=0.4$ , the angular frequency  $\omega=0.25$ , and the damping  $\gamma=0.75$ . Neighboring pendula are coupled via a discrete Laplacian, where  $k$  denotes the coupling strength. We have chosen free boundary conditions, i.e.,  $\theta_{0,m}=\theta_{1,m}$ ,  $\theta_{N,m}=\theta_{N+1,m}$ ,  $\theta_{n,0}=\theta_{n,1}$ ,  $\theta_{n,N}=\theta_{n,N+1}$ , and used a fourth-order Runge-Kutta routine with a time step  $dt=0.01$  to numerically integrate Eq. (1). We carefully checked that decreasing the time step to  $dt=0.001$  did not alter our results.

A very convenient measure that allows a quick visualization of the average global spatiotemporal behavior of the lattice is the average velocity

$$\sigma(jT) = \frac{1}{NM} \sum_{n=1}^{N \cdot M} \dot{\theta}_n(jT) \quad (2)$$

at multiple times of the driving period  $T=1/\omega$ . Using this quantity [15] to obtain a bifurcation diagram not only can ascertain if chaotic or periodic behavior is obtained, but in addition helps to identify the maximum period of a pattern: Computing  $\sigma(t)$  at each period  $t=jT$  of the driving will lead to a periodic sequence  $\sigma_1, \dots, \sigma_p, \sigma_1, \dots$  when transients have died out and a spatiotemporal pattern of periodicity  $p$

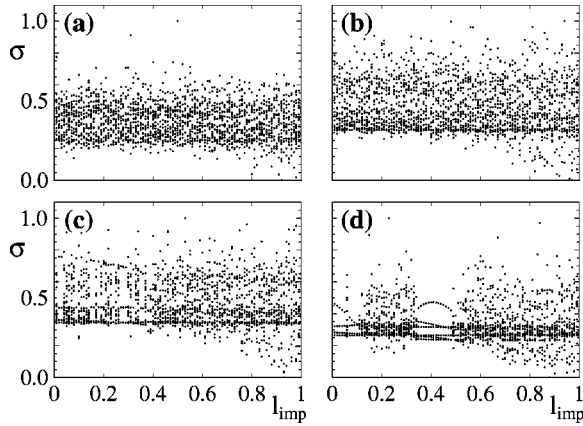


FIG. 1. Bifurcation diagram for a  $50 \times 50$  lattice of coupled pendula with length  $l_{n,m}=1$ . A single impurity with length  $l_{\text{imp}}$  is located at lattice site  $(25,25)$ . For each  $l_{\text{imp}}$ , the values of  $\sigma(151T), \dots, \sigma(170T)$  are shown, where  $T$  is the period of the driving. The coupling is (a)  $k=1$ , (b)  $k=2$ , (c)  $k=3$ , and (d)  $k=5$ . In (c) the first windows of synchronization can be observed, which enlarge for bigger couplings (d).

(“ $Pp$  attractor”) has emerged. In practice, we inspect the last 20 values of  $\sigma(jT)$  with  $j=1, \dots, 170$ , so that transients have died out. Thus,  $P20$  attractors or attractors of larger periodicity are not recognized as such but rather appear as chaotic attractors.

Applying this strategy to an isolated pendulum, a bifurcation analysis with respect to the pendulum length  $l$  was performed in Ref. [14]. This approach revealed that each isolated pendulum is chaotic for values  $l=1 \pm 0.002$  and that three more chaotic windows exist: Two narrow ones at  $l \approx 0.84$  and  $l \approx 0.52$ , and a broad one for  $l < 0.35$ . Thus we know whether a chosen pendulum with length  $l$  is chaotic or not. Furthermore, for the above chosen parameter values, it is known that pendula with  $l_{n,m} > 1$  and  $l_{n,m} < 1$  show libration and rotation, respectively, apart from the windows, where chaotic motion appears.

### III. RESULTS AND DISCUSSION

The simplest configuration of a 2D lattice described by Eq. (1) is that of a single impurity in a sea of identical chaotic pendula with length  $l_{n,m}=1$ . We fixed the lattice size to be  $50 \times 50$ , with the impurity located at site  $(25,25)$ , and made a bifurcation analysis with respect to the impurity length  $l_{\text{imp}}$  for various values  $k$  of the coupling. In Fig. 1, the obtained bifurcation diagrams for  $k=1,2,3,5$  are plotted versus  $l_{\text{imp}}$ . For convenience, we normalized  $\sigma$  to take on values in the unit interval  $[0,1]$ . Similarly to 1D arrays, we find that one impurity is able to organize the 2D arrays. However, our bifurcation analysis shows that the coupling constant has to be larger than  $k_{\text{cr}} \approx 3$ , whereas in the 1D case  $k \geq 0.1$  was sufficient [14] to produce spatiotemporal patterns. We would like to point out the appearance of a  $P4$  attractor for  $k=5, l_{\text{imp}} < 0.15$  in Fig. 1(d). Here an array of chaotic pendula is synchronized by a single impurity, which itself is chaotic, when isolated.

In order to illustrate the occurrence of this  $P4$  pattern in a

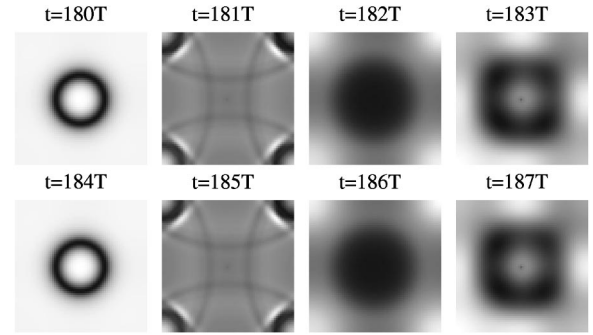


FIG. 2. Snapshots of  $\dot{\theta}_{n,m}$  for a  $64 \times 64$  lattice with  $l_{n,m}=1$ ,  $l_{\text{imp}}=l_{32,32}=0.1$ , and  $k=5$  at multiple times of the driving period  $T$ .

better way, we show in Fig. 2 a typical gray scale plot of the velocities  $\dot{\theta}_{n,m}$  as a function of the lattice coordinates  $(n,m)$ . The stroboscopic snapshots are taken with a time lag of one period of the driving  $T$ ; darker shading indicates higher velocity. In this example, we used  $64 \times 64$  oscillators having  $l_{n,m}=1$  and located an impurity of length  $l_{\text{imp}}=0.1$  in the middle of the lattice at  $(32,32)$ . The coupling constant is  $k=5$ . After some transient (not shown), the synchronization is maintained and a  $P4$  attractor is clearly visible. We neglect edge effects except to remark that they are strictly confined to the last few pendula near the boundaries. Moreover, they become very regular if the calculation is carried on for longer times.

In many applications, however, one is interested in the weak-coupling limit [16]. In this limit, our analysis shows that one impurity is not able to create spatiotemporal organization of a chaotic lattice. Therefore, it is meaningful to ask whether spatiotemporal patterns can emerge at all and under which conditions they may be obtained. To this end, we increase the number of impurities introduced in the lattice and investigate the importance of their geometrical arrangement as well as their concentration.

In Fig. 3(a), we report the  $P1$  pattern emerging for a  $128 \times 128$  lattice with coupling constant  $k=0.5$ , when 128 impurities were arranged along a line in the middle of the lattice, dividing it into two disjoint parts. The same behavior could be observed even for smaller couplings. We verified this for coupling constants as small as  $k_{\text{cr}}=0.1$ . Moreover, we found that increasing the size of the lattice to  $N=256$  (the limit of our computational capability), but maintaining the linelike geometry of impurities and the parameter values, did not affect the formation of a pattern. In all cases, we observed synchronization to a  $P1$  pattern after an initial transient. Thus, increasing the size of the lattice will not affect the pattern formation, although the percentage of the impurities will tend to zero in the limit of infinite systems. This indicates that the concentration of impurities is not of primary importance.

To test the influence of the special arrangement of impurities, we considered a  $128 \times 128$  lattice with  $k=0.5$  and 128 impurities of length  $l_{\text{imp}}=0.7$  located at random positions of the lattice. In all cases we have studied we obtained chaotic patterns. Even an increase of their concentration by more than a factor of 3 did not produce any spatiotemporal pattern.

It is thus natural to ask whether a line of impurities is the

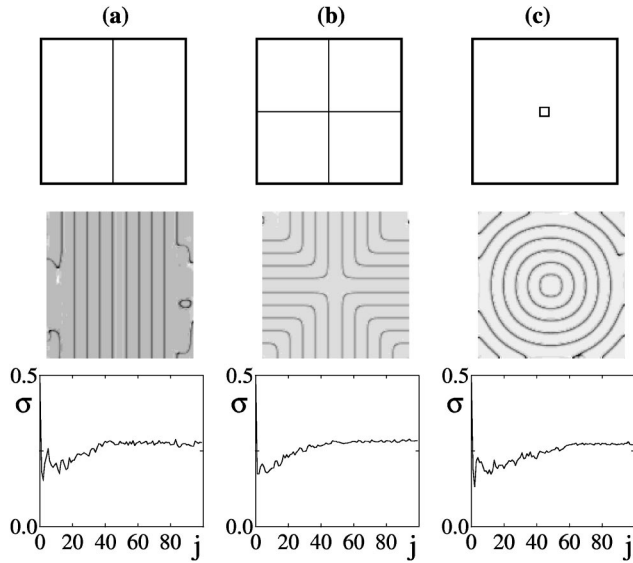


FIG. 3. Snapshots of  $\theta_{n,m}$  for a  $128 \times 128$  lattice with  $l_{n,m} = 1$ ,  $l_{\text{imp}} = 0.7$ , and  $k = 0.5$ . The impurities are positioned as indicated in the upper panel: (a) on a line along  $n = 64$ , (b) on a cross along the lines  $n = 64$  and  $m = 64$ , (c) on a square with  $(n, m) = (63, 63)$  the lower left and  $(66, 66)$  the upper right corner. In the lower panel, the corresponding  $\sigma(jT)$  is shown.

only geometry that can produce spatiotemporal patterns for relatively small values of the coupling constant. In Figs. 3(b) and 3(c), we report the  $P1$  attractors of a lattice of  $128 \times 128$  coupled pendula with lengths  $l_{n,m} = 1$ ,  $l_{\text{imp}} = 0.7$ , and coupling  $k = 0.5$ , where the impurities are arranged like a cross [Fig. 3(b)] or as a ring [Fig. 3(c)]. In both cases, the observed pattern geometries consist locally of stripes, as was also observed for the “line geometry” in Fig. 3(a).

What is the common geometrical feature of the above impurity configurations that allow them to control the chaotic lattice? From the above analysis, we draw the conclusion that it is sufficient for synchronization that the impurities divide the lattice into *at least* two disjoint subregions. In that way, the critical coupling needed to observe a spatiotemporal pattern is decreased by an order of magnitude. Reducing the coupling below  $k_{\text{cr}} \approx 0.1$ , however, suppresses the formation of spatiotemporal patterns even for these lattices. This finding is consistent with earlier investigations on 1D arrays, which revealed a critical coupling  $k \approx 0.1$ , below which no pattern formation could be observed. Furthermore, the observed  $P1$  pattern for the “line geometry” [Fig. 3(a)] is analogous to the 1D case, where the introduction of a single impurity caused the same topology of the array, i.e., a division into two disjoint sets, and a similar pattern was observed [14]. Thus, the results of the 1D case define the limiting  $k$  value also for the 2D lattice.

We finally examined the effect of disorder and the possibility of obtaining self-organization or frequency locking. For a  $128 \times 128$  lattice, we randomly varied the lengths of the pendula but restricted the range of the disorder such that each individual pendulum is chaotic, i.e.,  $l_{n,m} \in [0.998, 1.002]$ . We found that the emerging pattern was always chaotic for a large number of different realizations of disorder and initial conditions. The lacking synchronization can be observed in a

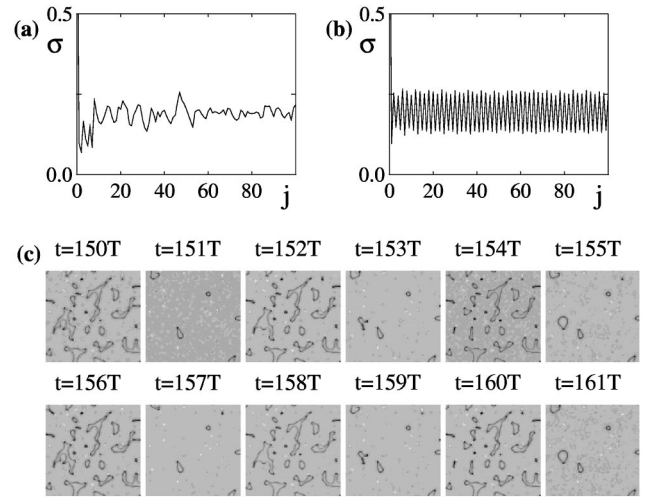


FIG. 4. (a) Chaotic sequence  $\sigma(jT)$  for a  $128 \times 128$  lattice ( $k = 0.5$ ) with  $l_{n,m} \in [0.998, 1.002]$ . (b) Periodic sequence  $\sigma(jT)$  for a  $128 \times 128$  lattice ( $k = 0.5$ ) with  $l_{n,m} \in [0.8, 1.2] \setminus [0.998, 1.002]$  revealing a  $P6$  pattern. (c) Snapshots at multiple periods  $T$  of the driving confirm the existence of a  $P6$  pattern as predicted in (b).

better way by inspecting  $\sigma(jT)$ , which does not show any periodicity [see Fig. 4(a) for an example]. If the range of disorder is increased to include also regular moving pendula, i.e.,  $l_{n,m} \in [0.8, 1.2]$ , self-organization is possible, in agreement with the findings of Ref. [12]. This can be understood by the observation that synchronization already occurs, when choosing the disorder from an interval of pendulum lengths associated with regular motion, i.e.,  $l_{n,m} \in [0.8, 1.2] \setminus [0.998, 1.002]$ . A particular example for this is shown in Figs. 4(b) and 4(c), where the occurrence of a  $P6$  pattern can be observed. Thus, taking the lengths from the entire interval  $l_{n,m} \in [0.8, 1.2]$  on average yields only 1% chaotic pendula, whose motion will be overdominated by the synchronizing regular ones, explaining the spatiotemporal pattern observed in Ref. [12].

#### IV. CONCLUSION

In conclusion, we have demonstrated that a lattice of chaotic pendula can be frequency-locked into a spatiotemporal pattern by introducing impurities in the lattice. In the strong-coupling limit, a single impurity can tame chaos. Decreasing the coupling constant requires more impurities in order to observe self-organization. In this case, the geometry of the impurity configuration plays an important role. Our results suggest that if the impurity configuration divides the lattice into at least two disjoint parts, then the coupling constant may be decreased without affecting the synchronization of the chaotic array. Moreover, the induced spatiotemporal patterns are then unaffected by the size of the lattice. Below the critical coupling  $k_{\text{cr}} \approx 0.1$ , no synchronization is observed. The value of this critical coupling is dictated by the minimum coupling, which leads to the formation of spatiotemporal patterns in the 1D case.

#### ACKNOWLEDGMENT

We are grateful to T. Gavrielides, V. Kovanis, A. Politi, and G. Tsironis for helpful discussions.

- [1] D. Amid, *Modelling Brain Function* (Cambridge University Press, Cambridge, UK, 1989); J. Hertz, A. Krogh, and R. Palmer, *Introduction to the Theory of Neural Computation* (Addison-Wesley, Redwood City, 1991).
- [2] A. Arneodo, J. Elezgaray, J. Pearson, and T. Russo, *Physica D* **49**, 141 (1991); G. K. Schenter, R. P. McRae, and B. C. Garrett, *J. Chem. Phys.* **97**, 9116 (1992).
- [3] G. Kozyreff, A. G. Vladimirov, and P. Mandel, *Phys. Rev. Lett.* **85**, 3809 (2000); H. G. Winful and L. Rahman, *ibid.* **65**, 1575 (1990); J. Terry, K. S. Thornburg, A. D. J. DeShazer, G. D. VanWiggeren, S. Zhu, and P. Ashwin, *Phys. Rev. E* **59**, 4036 (1999); A. Hohl, A. Gavrielides, T. Erneux, and V. Kovanis, *Phys. Rev. Lett.* **78**, 4745 (1997).
- [4] A. V. Ustinov, M. Cirillo, and B. Malomed, *Phys. Rev. B* **47**, 8357 (1993); K. Wiesenfeld, P. Colet, and S. Strongatz, *Phys. Rev. Lett.* **76**, 404 (1996).
- [5] S. H. Strogatz, C. M. Marcus, R. M. Westervelt, and R. E. Mirollo, *Physica D* **36**, 23 (1989).
- [6] E. N. Economou, *Green's Functions in Quantum Physics*, Springer Series in Solid State Physics Vol. 7 (Springer-Verlag, Berlin, 1979).
- [7] A. V. Ustinov, B. A. Malomed, and S. Sakai, *Phys. Rev. B* **57**, 11 691 (1998); O. M. Braun and Yu. S. Kivshar, *Phys. Rep.* **306**, 1 (1998); E. Nylund, K. Lindenberg, and G. Tsironis, *J. Stat. Phys.* **70**, 163 (1993).
- [8] J. F. Heagy, L. M. Pecora, and T. L. Carrol, *Phys. Rev. Lett.* **21**, 4185 (1995); J. F. Heagy, T. L. Carrol, and L. M. Pecora, *Phys. Rev. E* **50**, 1874 (1994).
- [9] L. M. Floria and J. J. Mazo, *Adv. Phys.* **45**, 505 (1996).
- [10] A. V. Ustinov, M. Cirillo, and B. A. Malomed, *Phys. Rev. B* **47**, 8357 (1993).
- [11] S. Pagano, M. P. Soerensen, R. D. Parmentier, P. L. Christiansen, O. Skovgaard, J. Mygind, N. F. Pedersen, and M. R. Samuelsen, *Phys. Rev. B* **33**, 174 (1986).
- [12] Y. Braiman, J. F. Lindner, and W. L. Ditto, *Nature (London)* **378**, 465 (1995); N. V. Alexeeva, I. V. Barashenkov, and G. P. Tsironis, *Phys. Rev. Lett.* **84**, 3053 (2000).
- [13] Y. Braiman, W. L. Ditto, K. Wiesenfeld, and M. L. Spano, *Phys. Lett. A* **206**, 54 (1995).
- [14] A. Gavrielides, T. Kottos, V. Kovanis, and G. P. Tsironis, *Phys. Rev. E* **58**, 5529 (1998); *Europhys. Lett.* **44**, 559 (1998).
- [15] There are a variety of related quantities that may be defined in a similar way. However, we use  $\sigma(jT)$  as a particular intuitive measure, which furthermore is easy to calculate.
- [16] H. G. Winful and L. Rahman, *Phys. Rev. Lett.* **65**, 1575 (1990).